Exp Brain Res
DOI 10.1007/s00221-009-2073-1

RESEARCH ARTICLE

Kinematic analysis of the human wrist during pointing tasks

Domenico Campolo · Domenico Formica · Eugenio Guglielmelli · Flavio Keller

Received: 4 August 2009 / Accepted: 24 October 2009

Abstract In this work, we tested the hypothesis that intrinsic kinematic constraints such as Donders' law are adopted by the brain to solve the redundancy in pointing at targets with the wrist. Ten healthy subjects were asked to point at visual targets displayed on a monitor with the three dof of the wrist. Three-dimensional rotation vectors were derived from the orientation of the wrist acquired during the execution of the motor task and numerically fitted to a quadratic surface to test Donders' law. The thickness of the Donders' surfaces, i.e., the deviation from the best fitting surface, ranged between 1° and 2°, for angular excursions from ±15° to ±30°. The results support the hypothesis under test, in particular: (a) Two-dimensional thick surfaces may represent a constraint for wrist kinematics, and (b) inter-subject differences in motor strategies can be appreciated in terms of curvature of the Donders' surfaces.

Keywords Donders' law · Intrinsic kinematic constraints · Rotational synergies · Wrist kinematics

D. Campolo (✉)
School of Mechanical & Aerospace Engineering,
Nanyang Technological University, 50 Nanyang Avenue,
Singapore 639798, Singapore
e-mail: d.campolo@ntu.edu.sg

D. Formica · E. Guglielmelli
Laboratory of Biomedical Robotics and Biomicrosystems,
Università Campus Bio-Medico di Roma, Via A. del Portillo, 21,
00128 Rome, Italy

F. Keller
Laboratory of Developmental Neuroscience,
Università Campus Bio-Medico di Roma, Via A. del Portillo, 21,
00128 Rome, Italy

Introduction

Studies on human motor control have demonstrated the existence of simplifying strategies adopted by the brain when dealing with kinematically redundant problems. Such strategies are often referred to as Donders' law for historical reasons, in relation to Donders' studies on the eye movements.

The eye can be considered as a center-fixed sphere rotated by the action of six (i.e., three agonist–antagonist couples) extraocular muscles providing three degrees-of-freedom (DOF) kinematics and allowing full mobility in the three-dimensional space of rigid body rotations, with limitations only in terms of range of motion. When looking at a visual target, infinite eye configurations exist corresponding to the same gaze direction but with different amount of ocular torsion.

Donders (1847) experimentally found that for a given steady gaze direction there is only one physiological eye orientation (Donders' Law) (Tweed and Vilis 1990), i.e., a two-dimensional constraint embedded into the three-dimensional space of eye configurations: a solution to redundancy.

Two decades later, Listing and Helmholtz went one step further, determining that such a two-dimensional surface is actually a plane: the eye assumes only those positions that can be reached from the primary position by a single rotation about an axis in the Listing's plane, which lies orthogonal to the gaze direction in the primary position (Listing's Law) (Tweed and Vilis 1990).

In the last 2 decades, Donders' and Listing's laws have been found to well represent intrinsic strategies of the motor control system during pointing tasks, executed via eye movements (both saccades and smooth pursuit), as well as head or arm movements (Hore et al. 1992),

Published online: 15 November 2009

(Gielen et al. 1997); the reader is referred to (Fetter et al. 1997) for a comprehensive collection of such works as well as to more recent papers such as (Liebermann et al. 2006) and references therein.

Remarkable similarities exist in terms of kinematics between the oculomotor system (extensively studied in literature) and the human wrist. The human wrist is in fact endowed with three DOF: prono-supination PS, flexion–extension FE, and radialulnar deviation RUD. While FE and RUD are anatomically confined within the wrist, the prono-supination is due to the articulated complex between elbow and wrist. The three rotations occur about approximately perpendicular axes (see Fig. 1). The RUD axis is typically 2–15 mm distally offset from the FE axis (Leonard et al. 2005).

So far, to the authors' knowledge, no evidence has been provided for the existence of simplifying strategies for redundancy of the human wrist kinematics during pointing tasks. In general, wrist kinematics is definitely much less explored than shoulder–elbow movements despite the fact that distally located on the upper limb and together with the hand, it is crucially instrumental to most of the activities of daily living. Restoring the lost distal functionality of the wrist/hand is of great interest to the neuro-rehabilitation community and very recently specific technologies for robot-mediated wrist rehabilitation have been proposed and validated in clinical trials (Krebs et al. 2007), (Masia et al. 2009), (Takahashi et al. 2008), (Gupta et al. 2008). Differently from previous shoulder–elbow robots, the design of which was based on the knowledge built up in the last decades about kinematics, dynamics and neural control behind reaching movements, wrist robots lack such a fundamental knowledge (Charles 2008). Moreover, whereas studies on wrist kinematics typically look at movements resulting from a combination of flexion–extension and radialulnar deviation (prono-supination is typically constrained, see (Charles 2008, Sec. 1.3, for a comprehensive review) we consider the full three DOF kinematics altogether.

Despite being a 'neglected' motor district, methods for the analysis of the three DOF wrist kinematics can take advantage of over a century of research on eye movements. In fact, at least in terms of kinematic redundancy, pointing tasks for the human wrist are similar to gazing tasks for the oculomotor system: the wrist is endowed with three DOF kinematics (flexion–extension, radial–ulnar deviation and pronation–supination), while for pointing tasks, only two DOF are required. Of course, profound differences also hold as the eye has a simpler muscle arrangement, while the wrist or the arm have to fulfil more functions and thus have more complex muscle geometry.

Pointing tasks towards visual targets (from/to a central target to/from peripheral ones) with the sole use of wrist kinematics can be guided via 'video games' as the one shown in Fig. 1. Such an approach was already proposed and validated for robot-mediated wrist motor therapy (Krebs and Hogan 2006; Krebs et al. 2007).

The objective of this paper is to present a method for studying intrinsic kinematic constraints of human wrist during pointing tasks and to report the experimental findings supporting the existence of Donders' Law for the human wrist.

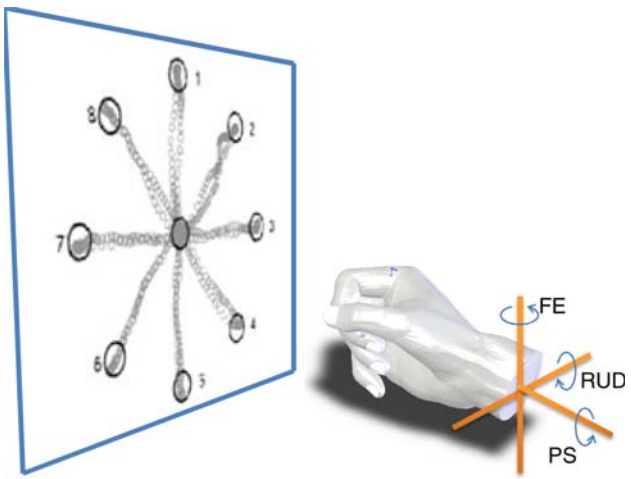

Fig. 1 Typical 'video game' for guiding a subject through pointing tasks: the subject is instructed to move the round cursor from the central position towards a peripheral position ('1', '2', …, '8'), randomly chosen by the software, and then back to the central position. A typical outcome of a experimental session is also superimposed (*smaller circles*)

Materials and methods

This section presents the proposed methodology, the experimental setup and the experimental protocol devised to test the hypothesis that intrinsic kinematic constraints, such as Donders' Law, can account for the geometric features of three-dimensional wrist movements during pointing tasks.

Mathematical background: representation of rotations

Rotations in the Euclidean space $\mathbb{R}^3$ can be described by the group of 3×3 orthonormal matrices $R \in \mathbb{R}^{3\times3}$ with determinant $+1$. Any orientation of a rigid body, with respect to a given reference, can be achieved via a single rotation about a fixed axis $\mathbf{v} \in \mathbb{R}^3$ through an angle $\theta \in [0, 2\pi)$ (Murray et al. 1994, Euler's Theorem). As such, a rotation matrix R can be seen as a mapping $R : \mathbb{R}^3 \rightarrow \mathbb{R}^3$ and represented in $\mathbb{R}^3$ (i.e., the same space it acts upon) via a rotation vector $\mathbf{r} = [r_x, r_y, r_z]^T \in \mathbb{R}^3$, which defines the

axis (parallel to $\mathbf{r}$ itself) and the amount of rotation ($\|\mathbf{r}\| = \tan(\theta/2)$). As shown in (Haslwanter 1995), for a generic rotation R, the corresponding rotation vector is:

$$\mathbf{r} = \frac{1}{1 + R_{1,1} + R_{2,2} + R_{3,3}} \begin{bmatrix} R_{3,2} - R_{2,3} \\ R_{1,3} - R_{3,1} \\ R_{2,1} - R_{1,2} \end{bmatrix} \quad (1)$$

where $R_{i,j}$ represents the (i, j) element of the matrix R. Just like rotation matrices, two rotation vectors $\mathbf{r}_1$ and $\mathbf{r}_2$ can be composed with the following non-commutative rule:

$$\mathbf{r}_1 \circ \mathbf{r}_2 = \frac{\mathbf{r}_1 + \mathbf{r}_2 + \mathbf{r}_1 \times \mathbf{r}_2}{1 - \mathbf{r}_1 \mathbf{r}_2} \quad (2)$$

where $\mathbf{r}_1 \times \mathbf{r}_2$ and $\mathbf{r}_1 \mathbf{r}_2$ represent the standard vector product and scalar product in $\mathbb{R}^3$, respectively.

For solving a pointing task, only two DOF would suffice. Examples of mechanical systems with two DOF are the Fick's and Helmholtz's gimbals, where the order of rotation ($\mathbf{r}_V = [0\,0\,r_z]^{\mathrm{T}}$ about the vertical axis and $\mathbf{r}_H = [0\,r_y\,0]^{\mathrm{T}}$ about the horizontal axis) is mechanically imposed by the structure of the system[1] :

$$\mathbf{r}_{\mathrm{Fick}} = \mathbf{r}_V \circ \mathbf{r}_H = [-r_y r_z\; r_y\; r_z]^{\mathrm{T}} \quad (3)$$

$$\mathbf{r}_{\mathrm{Helm}} = \mathbf{r}_H \circ \mathbf{r}_V = [+r_y r_z\; r_y\; r_z]^{\mathrm{T}}. \quad (4)$$

From previous equations, it is clear that the following *mechanical* constraints hold for the r_x component of the rotation vectors for the two gimbals:

$$\begin{array}{ll} r_x = -r_y r_z & (\mathrm{Fick}) \\ r_x = +r_y r_z & (\mathrm{Helmholtz}) \end{array} \quad (5)$$

Equations 5 are quadratic forms and each describes a surface in the three-dimensional space of rigid body orientations.

On the other hand, the existence of a two-dimensional manifold implementing, not a biomechanical but a neural constraint (Donders' law) for a three DOF system such as the human eye is remarkable, since it denotes a simplifying strategy of the motor system.

Subjects

Ten right-handed healthy subjects (8 male and 2 female, aged between 25 and 35 years old), with no history of neuromuscular disorders or previous wrist injuries, were asked to complete a series of pointing tasks with their right wrist. Right handedness for all subjects was verified by means of a standard test of laterality (Oldfield test) (Oldfield 1971), which was administered to the subjects before starting the experiments. Prior to the experiments, all subjects gave informed consent. Furthermore, the study was carried out along the principles laid down in the Helsinki Declaration.

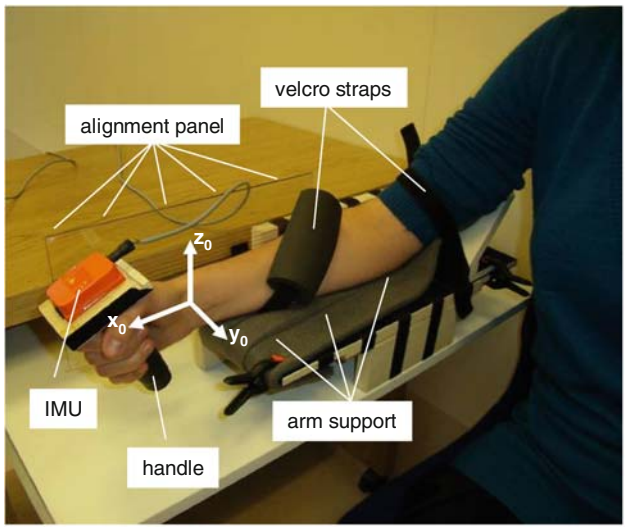

Fig. 2 Experimental apparatus for trials with the hand-held device. For each subject, the alignment panel, made of transparent plexiglass, is only used for the initial setup of the 'zero' position and removed during the trial execution

Experimental setup

Each subject was strapped to a chair and to an arm support by appropriate belts to minimize torso, shoulder and elbow movements, so that only wrist rotations were left unconstrained, as shown in Fig. 2. The orientation matrix R of the wrist was measured by means of an inertial magnetic unit (IMU, MTx-28A33G25 device from XSens Inc.; static orientation accuracy, <1°; bandwidth, 40 Hz) mounted on top of a hollow cylindrical handle (height, 150 mm; outer diameter, 50 mm; inner diameter, 35 mm; mass 120 g), which each subject was asked to grasp firmly[2] during the experiment. In what follows, such an apparatus is referred to as a *hand-held* device.

The IMU, connected to a PC, was configured to continuously acquire the sequence of orientation matrices R_i (relative to the ith sample) at a rate of 100 samples/s.

Before starting the trial, a 'zero' position for the wrist was defined by means of a vertical sliding panel (see Fig. 2), which was then removed for the execution of the

[1] The 'telescope' is an example of Fick's gimbal, where a (mobile) horizontal axis rotary joint is mounted on top of a (fixed) vertical axis rotary joint with the property that horizontal lines of the landscape will always appear horizontal to the spectating eye. A Helmholtz's gimbal consists of a (mobile) vertical axis rotary joint mounted on top of a (fixed) horizontal axis rotary joint.

[2] To avoid muscle fatigue and stiffening due to long time grasping, an elastic band was wrapped around the hand before each trial, soon after the definition of the 'zero' position of the wrist (see below). Besides reducing muscle fatigue and stiffening due to grasping, the wrapping elastic band also assured no slippage of the handle, so that wrist and handle device rotated as a single rigid body at all times.

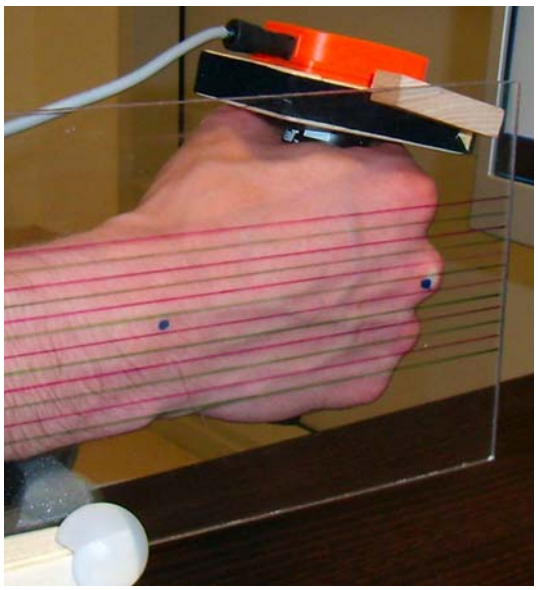

Fig. 3 Details of the sliding panel for the alignment of the wrist 'zero' position to its anatomical neutral position

trial for each subject. In particular, the panel is used to put the wrist in its anatomical neutral position as defined by the International Standard of Biomechanics (ISB) (Wu et al. 2005). In fact, it allows to univocally define the zero position for the FE and PS dof, by aligning the dorsal side of the hand with the forearm, and the zero position for RUD by aligning the third metacarpal of the hand with the central point between the ulnar and radial styloid processes. In Fig. 3 details of the sliding panel with the parallel lines used to easily align the RUD dof to its anatomical neutral position is shown.

With the wrist in its 'zero' position, a fixed reference frame $\{x_0, y_0, z_0\}$, also shown in Fig. 2, was defined as:

- z_0-axis: along the vertical direction (upwards);
- x_0-axis: horizontal, aligned with the forearm (forward);
- y_0-axis: horizontal and perpendicular to the forearm (leftward).

A second reference frame $\{x, y, z\}$ attached to the wrist (moving frame) was defined so as to coincide with the fixed reference frame when the wrist is in the 'zero' position. The previously described procedure for the definition of the 'zero' position has been used to define a fixed reference frame, which is directly related to an anatomical configuration of the wrist, so that all the subjects can perform the experiments starting from the same wrist configuration. This will make more reliable the comparison of the results among different subjects.

To reduce computational complexity, the 'zero' position was also selected as the 'home' position for the IMU, meaning that the coordinates of the x, y, and z axes with respect to the fixed frame $\{x_0, y_0, z_0\}$ could be determined as, respectively, the first, second and the third column of the matrix R_i. To this aim, a software reset procedure for the IMU device must be performed while the wrist is held still in the 'zero' position.

For a generic orientation R_i, the pointing vector, (always parallel with the moving x axis after the reset procedure) can then be determined as the first column of R_i:

$$\mathbf{n}_i = R_i[1\,0\,0]^{\mathrm{T}} \tag{6}$$

A computer screen was used to display the 'video game' according to the protocol below where (see Fig. 1) the position of a round cursor is determined, in real time, directly by the orientation of the subject's wrist. In particular, the screen was physically located on the vertical plane in front of the subject (the $y_0 - z_0$ plane) and the position of the cursor was determined by the projection of the pointing vector $\mathbf{n}_i$ onto the $y_0 - z_0$ plane. This would in fact reproduce the physical sense of pointing a laser beam at the screen, without involving geometric remapping between unrelated frames of reference[3].

The position of the cursor is given by the second and the third components of the vector $\mathbf{n}_i$.

Protocol

The session starts with the subject in the 'zero' position and, therefore, with the cursor projected onto the central position of the video game. The subject is then instructed to move the round cursor on the screen towards the peripheral positions randomly chosen by the software among '1', '2', …, '8' (see in Fig. 1) and then back to the central position. The random sequence is pre-computed before each trial. During the trial, all targets (peripheral and central) are always visible and, at any time, only one target is highlighted, indicating what target should be reached. The video game is interactive in the sense that once a highlighted target is reached by the cursor, the next target to be reached (according to the pre-computed random sequence) will be highlighted. One trial is completed after all the eight peripheral positions are reached.

For each subject, the whole experimental session is composed of four groups of five trials:

- the first group of five trials, referred to as 'learning trials', are used to make the subjects acquainted with the experimental setup and with the motor task to be performed. The data obtained from these trials have not been included in the statistical analysis of the results;
- the second group is composed of five trials in which the peripheral target positions can be reached by rotating

[3] As in the case of a computer mouse moved horizontally on the desk and producing vertical movements on the computer screen.

the wrist by only 15° (0.26 rad). These trials are also referred in this paper to as 'small circle trials';

- The third group requires a wrist rotation of 30° (0.52 rad) to get to the peripheral positions. These trials are named 'big circle trials';
- the fourth group has the peripheral target positions disposed on an ellipse, so that it is necessary to rotate the FE dof of 30° to reach targets 3 or 7, and to move the RUD dof of 15° to get to targets 1 or 5 (see Fig. 1). These trials are referred to as 'ellipse trials' in the rest of the text.

For a whole session, the 20 trials (5 trials × 4 groups) were performed in sequence, with only a 10 s pause between each trial. Since, especially for the 'big circle trials', large wrist rotations are required that might exceed a subject's biomechanical limit, before the session we instructed every subject to move but 'not to force' towards targets that seemed out of reach. For this reason, a time limit was set so that if a highlighted target could not be reached within 2 s, the next target would be automatically highlighted. With this time limit and considering the pauses between trials, the whole session would last no longer than 14 min.

These different tasks have been designed to test if some differences occur in motor strategies between movements close to the neutral position and wider movements; nevertheless, some targets of the big circle trials are close to or out of the limits of RUD range of motion. For this reason, since the natural range of motion of the wrist is not symmetrical [the ROM of FE dof is more than double with respect to the RUD (Li et al. 2005)], the ellipse trials have been implemented to allow subjects to span the whole natural range of motion without getting close to ROM limits.

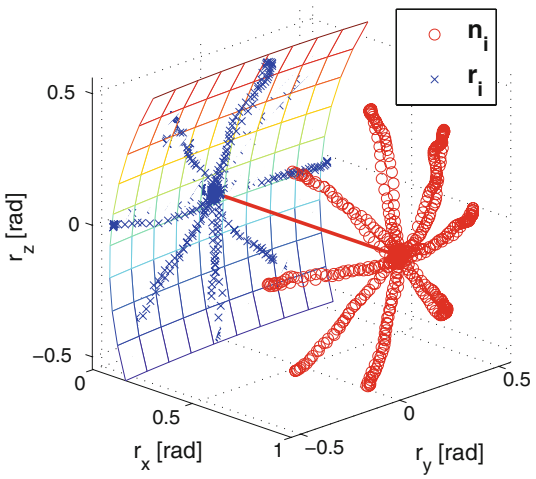

Fig. 4 Rotation vectors (*crosses*) are represented (in radians) in the three-dimensional space of the motor task together with the pointing vectors (*circles*). A two-dimensional quadratic surface (Donders' surface) fits the rotation vectors. The straight line represents the pointing direction when the wrist is in the 'zero' position

Data analysis

Given the sequence R_i relative to each trial, the sequence of rotation vectors $\mathbf{r}_i$ and the sequence of pointing vectors $\mathbf{n}_i$ were derived via Eqs. 1 and 6, respectively. As an example, both sequences of a single trial are plotted in Fig. 4.

It is worth here recalling the geometrical interpretation of $\mathbf{r}_i$: at any time t_i, the orientation R_i of the wrist can be achieved from the 'zero' position by a single rotation about the vector $\mathbf{r}_i$ of an angle $\theta_i = 2\arctan(\|\mathbf{r}_i\|)$. Such an interpretation allows representing rotations in the same three-dimensional space of the motor task. In Fig. 4, both the wrist pointing directions $\mathbf{n}_i$ (circles) and the rotation vectors[4] $\mathbf{r}_i$ (crosses) are represented. While the wrist pointing directions necessarily lie in a two-dimensional space[5], the three components r_{xi}, r_{yi} and r_{zi} of a rotation vector $\mathbf{r}_i$, in general, define points of a three-dimensional space. Remarkably, it can be observed that the rotation vectors tend to lie on a two-dimensional surface (Donders' Law), which can be well approximated by a plane near the 'zero' position.

Numerically, as in (Tweed and Vilis 1990), the sequence $\mathbf{r}_i = [r_{xi}\, r_{yi}\, r_{zi}]^{\mathrm{T}}$ was fitted to $\mathbf{r}^*{}_i = [r^*_{xi}\, r_{yi}\, r_{zi}]^{\mathrm{T}}$ where is r^*_{xi} is defined by a generic quadratic surface:

$$r^*_{xi} = C_1 + C_2 r_{yi} + C_3 r_{zi} + C_4 r^2_{yi} + 2C_5 r_{yi} r_{zi} + C_6 r^2_{zi} \qquad (7)$$

where the coefficients C_1, …, C_6 were determined via nonlinear least-squares fitting methods[6]. The first three coefficients (C_1, C_2 and C_3) define a plane, while the last three coefficients (C_4, C_5 and C_6) are related to the curvature of the fitted surface, see (Do Carmo 1976). In particular, the coefficient C_5 denotes the amount of twisting of a quadratic surface.

As in previous studies, the thickness of a Donders' surface is defined as the standard deviation of the fitting error between the sequence $\mathbf{r}_i$ and the best fitting surface. For a given set of fitting coefficients (C_1, …, C_6), the fitting error is defined as $r_{xi} - r^*_{xi}$. Obviously, thickness values

[4] A commonly adopted practice in literature, although rarely explicitly stated, is to represent rotation vectors or quaternions (Haslwanter 1995) with vectors of length θ_i (instead of $\tan(\theta_i/2)$ or $\sin(\theta_i/2)$) so that the amount of rotation as well as angular errors can be readily derived either in radians or degrees. Practically, these kinds of vectors do not differ much over the angular ranges of interest (Haustein 1989).

[5] Pointing vectors $\mathbf{n}_i$ are unit length vectors and therefore their end tips lie on a sphere as clear in Fig. 4.

[6] The function `nlinfit` in the MATLAB environment from MathWorks Inc. was used

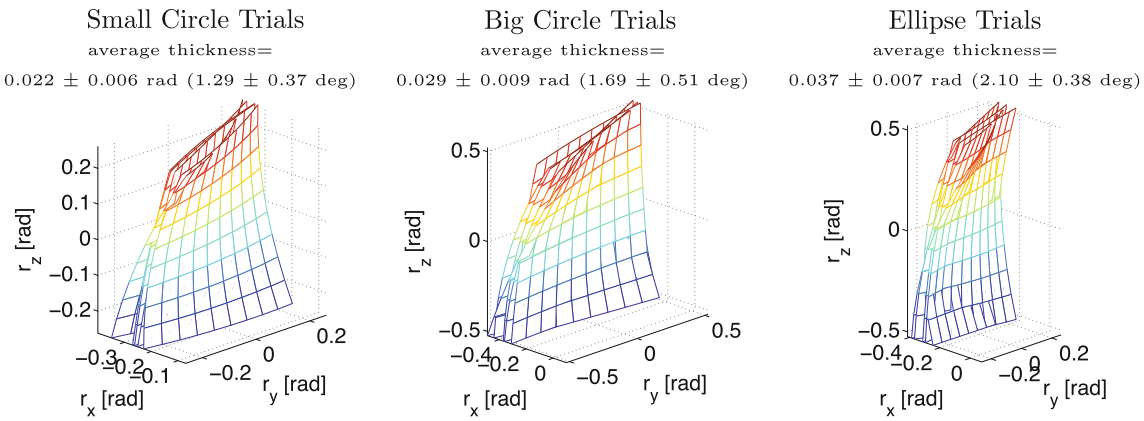

Fig. 5 Superimposed Donders' surfaces fitting the rotation vectors (in radians) relative to one representative subject for the different motor tasks ('*small circle*', '*big circle*' and '*ellipse*'), each of them composed of five trials. Thickness values (mean ± SD) are also reported

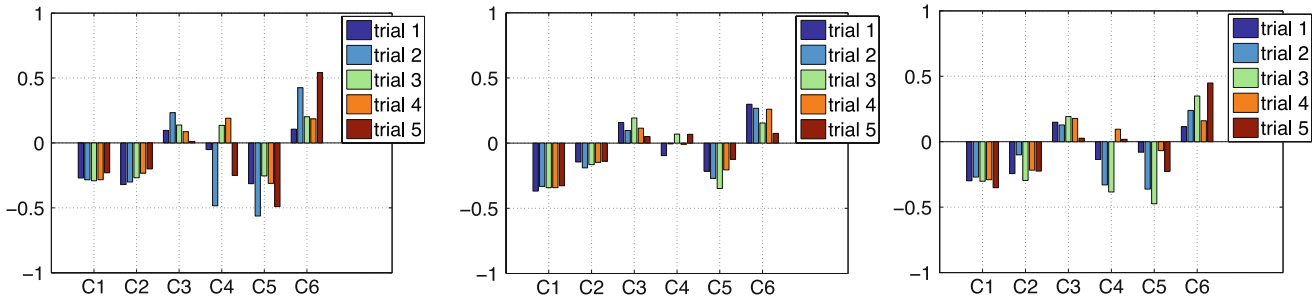

Fig. 6 Histogram of the C_1, …, C_6 coefficients, relative to one representative subject, fitting each of the five trials

quantify the goodness of fitting and indicate how much the rotation vectors tend to lie on the best fitting surface (Donders surface); low values of thickness indicate that a soft constraint (such as Donders' Law) apply to wrist kinematics during pointing tasks. To test whether a quadratic fitting is necessary or a linear fitting would suffice, a linear regression was also implemented on the same data set and thickness values for the two different regressions were compared.

Results

Data from each single trial were fitted with a generic quadratic surface as described in the previous section. Figure 5 presents the results relative to one representative subject in terms of Donders' surfaces, while Fig. 6 reports the histograms of the C_1, …, C_6 coefficients for each trial.

The 3D wrist rotations are well fitted by the Donders' surfaces as demonstrated by the low values of the thickness (around 2° or less), as also shown in Fig. 5. It should be noticed that each trial would last at most 32 s[7], which at 100 Hz sampling rate produces a maximum number of 3,200 orientation samples per trial. All the trials for all the subjects consisted of at least 765 samples (most of the trials had more than 1,000 samples), over which the thickness was computed.

The visual result of the 'video game', shown in Fig. 7, is the 2D outcome of subject's movements and corresponds to the trajectory of the cursor on the screen, i.e., the projection of the pointing vector on the vertical plane in front of the subject. As such, it carries less information than 3D representation of the wrist orientation.

In Table 1 mean and standard deviation of thickness values averaged for all subjects are reported for different trials ('small circle', 'big circle' and 'ellipse'). In particular, a comparison between the generic quadratic fitting and a simple linear regression is given: as expected; the difference between the linear and the quadratic regression are not statistically significant for the small circle trials, meaning that for movements close to the neutral position the Donders' surfaces can be well approximated by a plane. Nevertheless, for wider movements, the quadratic fitting resulted in a statistically significant reduction of thickness of about 15%. It is worth noting that the mean value of the thickness, averaged on 150 trials (15 trials × 10 subjects), is 1.46° ± 0.69° (SD) and is in line with deviations

[7] Maximum trial time = 2 s (time limit for each movement) × 2 kinds of movements (center-out and return) × 8 targets.

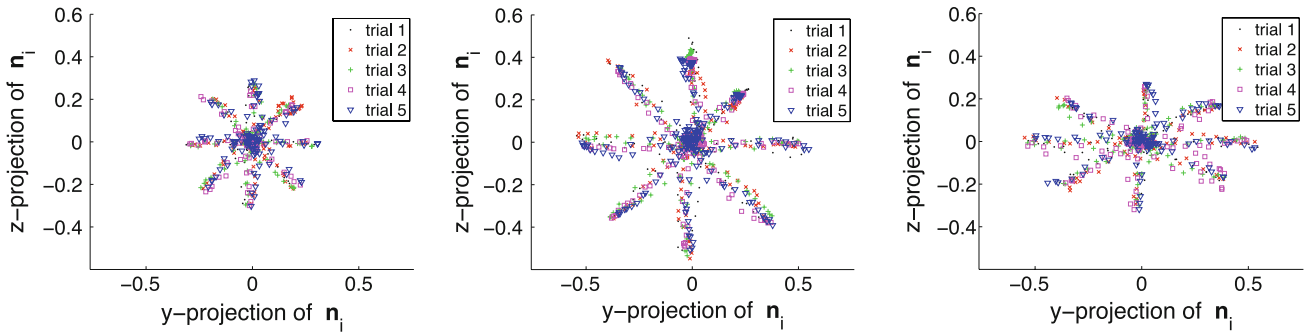

Fig. 7 Superimposed visual outcomes, relative to one representative subject, of the five motor tasks

Table 1 Overview of the thickness values (mean ± SD) for all the subjects, with a comparison between a linear fitting and a generic quadratic fitting

	Linear thickness	Quadratic thickness	Difference	*p* value
Small circle	0.017 ± 0.006 rad	0.015 ± 0.006 rad	0.002 rad	0.074
	(1.02 ± 0.37°)	(0.89 ± 0.34°)	(0.13°) (− 13%)	
Big circle	0.042 ± 0.015 rad	0.035 ± 0.012 rad	0.007 rad	0.016*
	(2.40 ± 0.86°)	(2.02 ± 0.67°)	(0.38°) (− 16%)	
Ellipse	0.030 ± 0.010 rad	0.026 ± 0.008 rad	0.004 rad	0.017*
	(1.74 ± 0.57°)	(1.48 ± 0.47°)	(0.26°) (− 15%)	
Overall	0.030 ± 0.015 rad	0.025 ± 0.012 rad	0.004 rad	0.005*
	(1.71 ± 0.85°)	(1.46 ± 0.69°)	(0.25°) (− 15%)	

Statistically significant differences are indicated with a star in the *p* value column

found in the oculomotor system (Tweed and Vilis 1990) or in the upper limb experiments (Liebermann et al. 2006).

As qualitatively suggested by Fig. 5, for the same subject, Donders' surfaces seem to maintain similar curvature across the three different sets of movements. On the other hand, when experimental results from all the ten subjects are compared as in Fig. 8 (where surfaces relative to different subjects are superimposed, each surface representing the averaged over five trials) and Fig. 9, larger between-subjects variability can be noticed. This might be indicative of subject-specific features for each subject, i.e., a different motor strategy, throughout the execution of the motor tasks, which could be encoded in terms of curvature of the Donders' surfaces. To test whether this was really the case, we performed a multivariate analysis of variance (MANOVA) on the curvature of the surfaces to evaluate within-subject and between-subjects variability.

The curvature of generic surfaces can be characterized by two invariants, namely the Gaussian curvature (K) and the *mean curvature* (H) (Do Carmo 1976). For the specific case of quadratic surfaces (see Appendix for details), we computed and evaluated both the invariants (K_0 and H_0) at the origin of the surface (i.e., at $r_y = 0$, $r_z = 0$) and performed MANOVA tests using the two-dimensional vector [K_0 H_0] as multivariate dependent variable.

Such tests are summarized in Table 2 where the main result of each test is determined by the value of D, which is an estimate of the dimension of the space containing the group means[8]. In Table 2, the *p* values, the Wilks' Lambda statistic values of the test are reported. For completeness of information, also the post hoc power values[9] are reported, although the use of post hoc power analysis is controversial (Hoenig and Heisey 2001; Bacchetti 2002).

Within-subject MANOVA showed that, for each subject, the means of the multivariate vector [K_0 H_0] do not differ (in a statistical sense) across the three different sets of movements, i.e., the Donders surfaces are curved in the same way irrespective of the range of motion requested by

[8] The MANOVA tests are performed using the MATLAB function `manova1`; it tests the null hypothesis that the means of each group are the same *n*-dimensional multivariate vector and that any difference observed in the sample X is due to random chance. If $D = 0$, there is no evidence to reject that hypothesis. If $D = 1$, then you can reject the null hypothesis at the 5% level, but you cannot reject the hypothesis that the multivariate means lie on the same line. Similarly, if $D = 2$ the multivariate means may lie on the same plane in *n*-dimensional space, but not on the same line, and so on. The maximum value of *D* is the dimension of the multivariate vector (i.e., 2, in our case).

[9] Computed with `powerMAOV1` (Trujillo-Ortiz and Hernandez-Walls 2003)

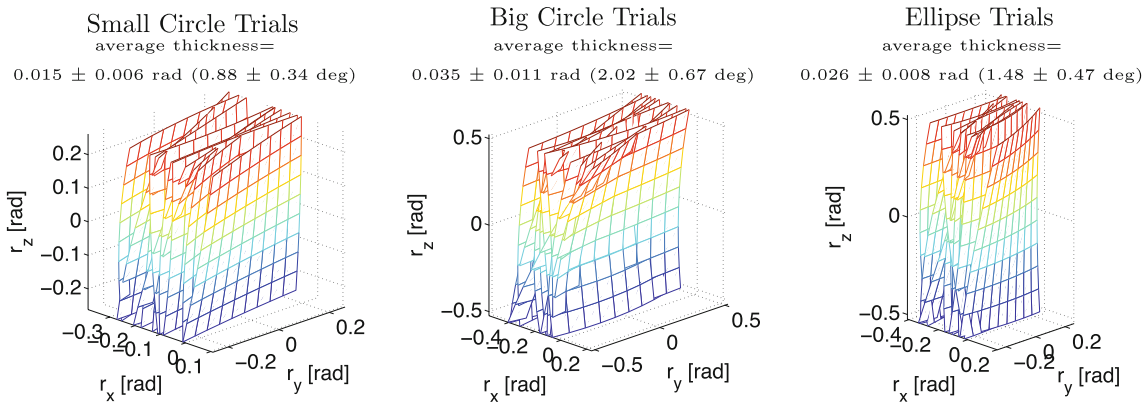

Fig. 8 Superimposed Donders' surfaces, averaged over the five trials, fitting the rotation vectors (in radians) relative to all subjects for all motor tasks ('*small circle*', '*big circle*' and '*ellipse*')

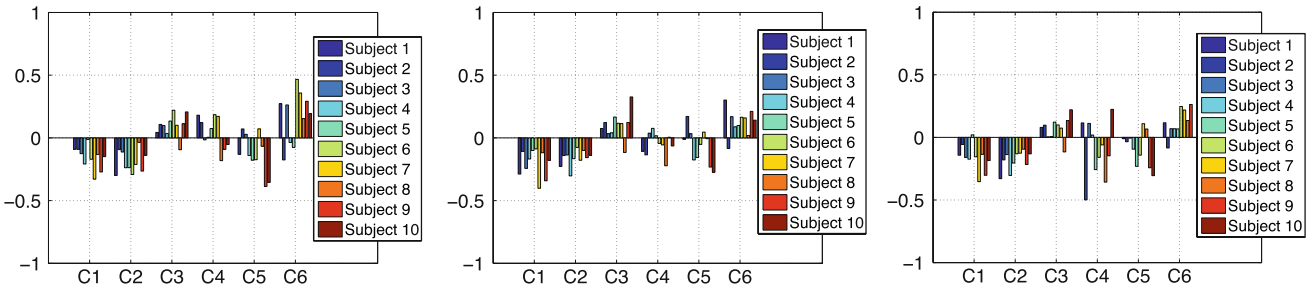

Fig. 9 Histogram of the C_1, …, C_6 coefficients averaged for five trials for each subject. Thickness values (mean ± SD) are also reported

Table 2 Summary table for the MANOVA tests performed with the multivariate vector [K_0 H_0] as dependent variable. In the within-subjects tests, for each subject, the effect of the three types of movements (Groups) was analyzed

Within subjects	No. groups	Tot. no. of data	D	p values for '$D = 0$'/'$D = l$'	Wilks' lambda	Post-hoc power
Sbj 1	3	15	0	0.3036/0.2588	0.6562/0.8951	0.40/0.12
Sbj 2	3	15	1	0.0114/0.5745	0.3238/0.973	0.93/0.07
Sbj 3	3	15	1	0.0023/0.1971	0.2358/0.8653	0.99/0.15
Sbj 4	3	15	0	0.3688/0.317	0.6889/0.9166	0.35/0.10
Sbj 5	3	15	0	0.4528/0.3942	0.7269/0.9388	0.30/0.09
Sbj 6	3	15	1	0.0497/0.0807	0.4377/0.767	0.77/0.25
Sbj 7	3	15	0	0.1961/0.2676	0.5914/0.8986	0.51/0.12
Sbj 8	3	15	0	0.3671/0.3101	0.6881/0.9143	0.35/0.11
Sbj 9	3	15	1	0.009/0.3939	0.3084/0.9387	0.94/0.09
Sbj 10	3	15	0	0.3554/0.5002	0.6825/0.9613	0.36/0.07
Between subjects	10	150	2	0/0.00004	0.4266/0.7874	1/0.98

For the between-subjects tests, the ten subjects were used as independent variables (10 groups). The multivariate hypotheses are '$D = 0$', '$D = 1$'. For such hypotheses, the relative p values, Wilk's Lambda and post hoc power are reported

the task. In particular, MANOVA tests using single subject trials as independent variable showed that in most cases, there was no evidence to reject the null hypothesis that the means of each group were the same two-dimensional multivariate vector ($D = 0$); in the rest of the subjects, the multivariate means lay on the same one-dimensional space ($D = 1$).

Between-subjects MANOVA was performed using subjects as independent variable and showed that inter-subjective differences in terms of curvature of Donders' surfaces are statistically significant (in a multivariate sense): subjects have a statistically significant effect on the [K_0 H_0] coefficients (their mean vector values span a full two-dimensional space, i.e., $D = 2$).

Table 3 Each row reports the values of the C_1, …, C_6 coefficients and the thickness averaged over 15 trials (mean ± SD) for each subject

Subjects	C_1 [rad]	C_2	C_3	C_4 [rad^{-1}]	C_5 [rad^{-1}]	C_6 [rad^{-1}]	Thickness [rad] (°)
1	−0.174 ± 0.090	−0.285 ± 0.068	0.066 ± 0.035	0.063 ± 0.205	−0.051 ± 0.083	0.230 ± 0.144	0.027 ± 0.016 (1.52 ± 0.94)
2	−0.085 ± 0.029	−0.138 ± 0.051	0.109 ± 0.043	−0.171 ± 0.323	0.069 ± 0.191	−0.115 ± 0.102	0.022 ± 0.011 (1.28 ± 0.64)
3	−0.176 ± 0.058	−0.129 ± 0.043	0.045 ± 0.052	0.044 ± 0.161	0.019 ± 0.133	0.167 ± 0.126	0.027 ± 0.008 (1.52 ± 0.48)
4	−0.183 ± 0.033	−0.282 ± 0.076	0.027 ± 0.034	0.033 ± 0.097	−0.137 ± 0.072	0.040 ± 0.131	0.020 ± 0.009 (1.17 ± 0.51)
5	−0.031 ± 0.076	−0.203 ± 0.066	0.141 ± 0.043	−0.055 ± 0.271	−0.188 ± 0.090	0.030 ± 0.129	0.021 ± 0.006 (1.23 ± 0.34)
6	−0.138 ± 0.055	−0.166 ± 0.113	0.145 ± 0.066	−0.006 ± 0.195	−0.123 ± 0.116	0.293 ± 0.155	0.025 ± 0.012 (1.44 ± 0.71)
7	−0.361 ± 0.042	−0.172 ± 0.051	0.096 ± 0.031	0.018 ± 0.222	0.076 ± 0.115	0.245 ± 0.141	0.026 ± 0.014 (1.50 ± 0.79)
8	−0.130 ± 0.027	−0.075 ± 0.059	− 0.108 ± 0.047	−0.256 ± 0.226	−0.001 ± 0.170	0.108 ± 0.106	0.027 ± 0.012 (1.53 ± 0.71)
9	−0.305 ± 0.037	−0.213 ± 0.066	0.123 ± 0.064	−0.078 ± 0.201	−0.287 ± 0.146	0.255 ± 0.136	0.029 ± 0.009 (1.69 ± 0.51)
10	−0.171 ± 0.062	−0.137 ± 0.037	0.251 ± 0.075	0.036 ± 0.255	−0.311 ± 0.167	0.111 ± 0.138	0.030 ± 0.016 (1.71 ± 0.95)
Overall	−0.176 ± 0.106	−0.181 ± 0.090	0.091 ± 0.101	−0.036 ± 0.238	−0.094 ± 0.185	0.137 ± 0.176	0.025 ± 0.012 (1.46 ± 0.69)

Finally, for each subject, the values of the C_1, …, C_6 coefficients (as well as of the thickness) averaged over the 15 trials are reported in each row of Table 3 and used to define an averaged Donders' surface. Figure 10 shows ten superimposed averaged surfaces, one for each subject, as well as the averaged coefficients represented in the form of a histogram.

Discussion

The main goal of this study was to verify that Donders' Law holds during pointing tasks performed with the wrist. We found that during the execution of two-dimensional pointing tasks with the wrist, the distribution of three-dimensional rotation vectors (describing the wrist configuration) is well fitted to two-dimensional surfaces. For each fitting surface, the thickness (i.e., the standard deviation of all data points from the surface itself) ranged between 1 and 2° for angular excursions from 15° to 30°, in line with previous findings on eye movements and other motor districts.

Donders' Law is a particular form of motor synergy used by the CNS to simplify problems where kinematic redundancy is involved. The human motor system often needs to cope with kinematic redundancies as we generally have many more degrees of freedom than necessary to fulfil the requirements of everyday tasks. The coordination of kinematically redundant systems, first formulated by Bernstein (1967) as the redundancy problem, is a central issue for motor planning and motor control.

At present, the characteristics of motor planning and motor control behind 2D (planar) movements are fairly understood while, when it comes to more complex 3D movements, currently available motor theories fail to fully explain experimental data (Gielen 2009). The only exception is in the oculomotor domain (also three-dimensional), where Donders' Law was first formulated in 1847, then better specified in the form of Listing's Law and confirmed by all successive studies until now. As also highlighted by Gielen (2009), one possible explanation is that the oculomotor system is devoted to only one single motor-perceptual task, i.e., directing gaze, while for the human arm the brain might switch among different strategies to accomplish different tasks.

For tasks such as pointing with the wrist, eye–hand coordination is essential for a correct execution. Eye–hand coordination involves multiple frames of references and it was shown that the computation of the error vector between the target and the hand[10], which is essentially a 2D retinal error, may first occur in a gaze-centred frame

[10] Also when the hand is not visible.

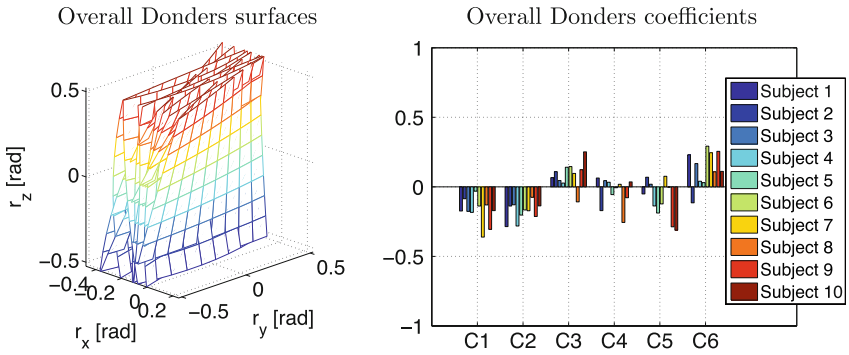

Fig. 10 Experimental data relative to all the 15 trials for each subject. *Left* superimposed Donders' surfaces fitting the rotation vectors (rad) from ten subjects (each surface describes the average outcome from 15 trials). *Right* histograms of the C_1, …, C_6 coefficients (averaged on 15 trials) relative to the 10 subjects

(Buneo et al. 2002). Further to this, a crucial early step was highlighted for the generation of accurate visually guided reaching (Blohm and Crawford 2007): the 2D retinal error needs to be first transformed into a 3D motor error and then projected through a series of roto-translations (involving coordinate transformations such as eye-in-head and head-on-shoulder) to a shoulder-centred frame for the limb muscles to implement the intended movement. Such a 3D motor error involves extraretinal information such as eye rotations and in particular embeds the Listing's law for the eyes.

Hepp (1990) already showed in abstract terms how a 2D retinal information can be used to generate a motor plan for 3D ocular saccades, basically consisting of a single fixed axis rotation, once the initial eye orientation is known and in compliance with Listing's law. Such an algorithm was then extended to explain concurrent coordination of eye, head and arm. In particular, Hepp et al. (1992) showed how, at least for restricted angular ranges, the coordination of the nine-dimensional system formed by three *rotational* subsystems (namely: the eye, the head and the arm, each being three-dimensional) was in fact reduced to a two-dimensional problem by operating on three approximately parallel Listing's planes, one for each subsystem. Furthermore Hepp et al. (1992) also found that such planes were workspace-centred, i.e., did not vary significantly when the body was rotated with respect to the workspace. Such results were also found to be in line with neurophysiological data from Caminiti et al. (1990) on the directional coding of cortical neurons related to arm movements, which on average rotates almost by the same amount as the centre of the workspace.

Taken altogether, the above considerations are consistent with the hypothesis that motor synergies are centrally planned at the level of kinematics, as already known for arm reaching movements (Shadmehr and Mussa-Ivaldi 1994). In particular, for rotational synergies, a highly optimized oculomotor synergy such as Listing's law is already available to the CNS as a solution to redundancy and might be 'projected' onto other rotational domains, e.g., the wrist.

While kinematics might be centrally planned by the CNS, the final movement execution would still be subject to the whole system biomechanics. Charles (2008) found that pointing movements performed with the wrist display significantly more path curvature than planar reaching movements performed with the arm. His findings support the hypothesis of an 'imperfect peripheral execution' likely due to biomechanical effects such as wrist muscle stiffness. Elastic properties of wrist muscles/tendons (especially if combined with the biomechanical limits of large wrist excursions) could be responsible for the quadratic rather than planar nature of the experimentally derived Donders' surfaces (see below).

The hypothesis of imperfect peripheral execution could also explain reported violations of Donders' law for the arm (Soechting et al. 1995), (Gielen et al. 1997) where, differently from the case of eye and wrist movements[11], for arm movements the effects of inertia and gravity might play an important role.

Linear versus quadratic fitting Similarly to the case of head and limbs movements, we also found that, especially for larger angular excursions of the tasks, Donders' law for the wrist is better represented by curved and twisted surfaces rather than a plane. In particular, as shown in Table 1, in the case of small circles (i.e., 15° angular excursions) the difference between linear (i.e., a plane) and quadratic (i.e., curved surface) fitting is close to significance ($p = 0.074$). Such differences become statistically significant when larger angular excursions are considered (large circles and ellipses). This is indicative that curvature of surfaces might reflect further workspace-related biomechanical constraints. This is in line with (Hore et al. 1992), where the existence of a Donders' law for the straight arm during pointing tasks was verified and where the resulting Fick-like curved surfaces were associated with a neurally imposed strategy to efficiently work against gravity.

[11] Especially in our experiment where all upper limb degrees of freedom but the three DOF of the wrist were constrained.

A possible example of such biomechanical constraints could be the elastic field generated by muscle stiffness. In fact, recent studies (Formica et al. 2009) showed that wrist stiffness in FE and RUD dof is not isotropic, causing an asymmetric energetic field in which a healthy subject moves his wrist. This yields that some movement directions in the FE-RUD space have higher impedance than others. One could speculate that human brain implements motor synergies, such as Donders' law, to allow the hand to move along paths of minimum impedance.

Furthermore, nonlinear features such as the curvature and twisting of the surfaces are indicative of subject-specific features, as curvature and twisting coefficients display much greater between-subject than within-subject variability. In particular, the MANOVA test confirms that these three curvature coefficients can be considered as the same vector for the 15 different trials of each subject, while they vary among different subjects.

Potential impact for neuro-rehabilitation The word 'synergy' has assumed different meanings within different scientific communities. In clinical neuro-rehabilitation, particularly for patients suffering from acute and focal CNS lesions (i.e., stroke), motor synergies play a negative role and are typically defined as stereotyped movements of the entire limb that reflect loss of independent joint control and limit a person's ability to coordinate her/his joints in flexible and adaptable patterns, thereby precluding optimal performance for many functional motor tasks. Thus, they are often considered as a form of impairment and the ability to 'extinguish' pathological synergistic movements is regarded as a goal of rehabilitation and pharmacological therapies (Dipietro et al. 2007).

Two main approaches to the degrees-of-freedom problem can be recognized in literature:

- *Optimization-based approaches* start from an a priori hypothesis and propose minimum principles in which a global cost function is assumed to be minimized by the CNS, leading thus to optimal behaviour which also solves the redundancy problem. Main theories are minimum-effort, minimum-jerk (Uno et al. 1989), minimum-torque change (Harris and Wolpert 1998), minimum-variance, (Harris and Wolpert 1998), uncontrolled manifold (UCM) (Scholz and Schoner 1999; Latash et al. 2007).
- *Phenomenological approaches* seek invariants at the level of measurable movement variables and give rise to empirical laws such as Donders'/Listing's law, Fitt's law, isochrony (Viviani and Schneider 1991), linearly related joint velocities (Soechting and Terzuolo 1987), 'two-third power law' (Lacquaniti et al. 1983).

While the former are motor control theories, which attempt to explain the phenomena, the latter are empirical and descriptive, therefore more operative.

The proposed method for assessing Donders' law for the human wrist can find direct application in clinical practice, in particular for functional assessment. In fact, pointing tasks such as the ones described in this paper approach were already proposed and validated for robot-mediated wrist motor therapy (Krebs and Hogan 2006; Krebs et al. 2007). Therefore, without major changes in the protocol, the quantitative assessment of Donders' law could be just 'added on' to benchmark atypical synergies and their change over time in post-stroke patients.

Analyzing the 3D rotation vectors (Fig. 6, top row), which fully describe the configuration of the wrist, rather than just looking at the two-dimensional projected outcomes (Fig. 6, bottom row) of the pointing task, provides an added value. As shown in Campolo et al. 2008, 2009 while between-subjects differences, or subject-specific features, can be appreciated in the 3D representation of the task, the same differences are not evident in the two-dimensional projection of the pointing task, meaning that it could not be possible to assess such differences by just looking at two-dimensional representations of the task.

This clearly may have a profound impact, for example, in functional assessment where the therapist typically evaluates two-dimensional projection of the tasks, especially considering that Donders' law is an adaptive law, which could be potentially used as an indicator of motor efficiency (Wong 2004).

Acknowledgments This work was partly funded by a grant from the European Union under the 6th framework, FP6-NEST/ADVENTURE program (TACT project, contract no. 015636).

Appendix: Computing curvature

The material in this appendix can be found in any differential geometry textbook, in particular (Do Carmo 1976). For the benefit of the reader, it is here reported in a notation, which is consistent with the rest of the paper.

Given a generic surface $r_x = f(r_y, r_z)$, the Gaussian and mean curvature can be determined as:

$$K = \frac{f_{yy}f_{zz} - f_{yz}}{\left(1 + f_y^2 + f_z^2\right)^2}$$

$$H = \frac{(1 + f_z^2)f_{yy} - 2f_y f_z f_{yz} + (1 + f_y^2)f_{zz}}{\left(1 + f_y^2 + f_z^2\right)^{3/2}}$$

where f_y and f_z are the first order partial derivative of f with respect to r_y and r_z (respectively) and, similarly, f_{yy}, f_{zz}, and f_{yz} are the second order partial derivatives.

For the case of interest, $f(r_y, r_z)$ is a generic quadratic function:

$$f(r_y, r_z) = C_1 + C_2 r_y + C_3 r_z + C_4 r_y^2 + 2C_5 r_y r_z + C_6 r_z^2$$

and the partial derivatives are $f_y = C_2 + 2C_4\, r_y + 2C_5\, r_z$; $f_z = C_3 + 2C_5\, r_y + 2C_6\, r_z$; $f_{yy} = 2C_4$; $f_{zz} = 2C_6$; $f_{yz} = 2C_5$.

When evaluated at the origin ($r_y = 0$, $r_z = 0$), the Gaussian and mean curvatures become, respectively,

$$K_0 = \frac{4C_4C_6 - 4C_5^2}{\left(1 + C_2^2 + C_3^2\right)^2}$$

$$H_0 = \frac{(2 + 2C_3^2)C_4 - 4C_3C_2C_5 + (2 + 2C_2^2)C_6}{\left(1 + C_2^2 + C_3^2\right)^{3/2}}$$

References

Bacchetti P (2002) Peer rewiew of statistics in medical research: the other problem. Br Med J 324:1271–1273

Bernstein N (1967) The co-ordination and regulation of movements. Pergamon Press, Oxford

Blohm G, Crawford JD (2007) Computations for geometrically accurate visually guided reaching in 3-D space. J Vis 7(5):4,1–22

Buneo CA, Jarvis MR, Batista AP, Andersen RA (2002) Direct visuomotor transformations for reaching. Nature 416:632–636

Caminiti R, Johnson PB, Urbano A (1990) Making arm movements within different parts of space: dynamic aspects in the primate cortex. J Neurosci 10:2039–2058

Campolo D, Accoto D, Taffoni F, Guglielmelli E (2008) On the kinematics of human wrist during pointing tasks with application to motor rehabilitation. In: Proceedings of the IEEE International Conference on Robotics and Automation, Pasadena, CA, USA, pp 1318–1323

Campolo D, Accoto D, Formica D, Guglielmelli E (2009) Intrinsic constraints of neural origin: assessment and application to rehabilitation robotics. IEEE Trans Robot 25:492–501

Charles S (2008) It's all in the wrist: a quantitative characterization of human wrist control. Dissertation, Massachusetts Institute of Technology, USA

Dipietro L, Krebs HI, Fasoli SE, Volpe BT, Stein J, Bever C, Hogan N (2007) Changing motor synergies in chronic stroke. J Neurophysiol 98:757–768

Do Carmo MP (1976) Differential geometry of curves and surfaces. Prentice Hall, New Jersey

Donders FC (1847) Beitrag zur Lehre von den Bewegungen des menschlichen Auges. Holland Beitr Anat Physiol Wiss 1:104–145

Fetter M, Haslwanter T, Misslich H, Tweed D (eds) (1997) Three-dimensional kinematics of the eye, head and limb movements. Harwood, Amsterdam

Formica D, Krebs HI, Charles SK, Zollo L, Guglielmelli E, Hogan N (2009) Passive wrist joint stiffness estimation, J Neurophysiol (accepted)

Gielen CCAM (2009) Review of models for the generation of multi-joint movements in 3-D. In: Sternad D (ed) Progress in motor control. Springer, Berlin

Gielen CCAM, Vrijenhoek EJ, Flash T, Neggers SFW (1997) Arm position constraints during pointing and reaching in 3D. J Neurophysiol 78: 1179–1196

Gupta A, O'Malley M K, Patoglu V, Burgar C, (2008) Design, control and performance of ricewist: a force feedback exoskeleton for wrist rehabilitation and training. Int J Rob Res 27:233–251

Harris CM, Wolpert DM (1998) Signal-dependent noise determines motor planning. Nature 394:780–784

Haslwanter T (1995) Mathematics of three-dimensional eye rotations. Vision Res 35:1727–1739

Haustein W (1989) Considerations on Listing's Law and the primary position by means of a matrix description of eye position control. Biol Cybern 60:411–420

Hepp K (1990) On Listing's law. Commun Math Phys 132:285–292

Hepp K, Haslwanter T, Straumann D, Hepp-Reymond M-C, Henn V (1992) The control of arm, gaze and head by. Listing's law. In: Caminiti R, Johnson PB, Burnod Y (eds) Control of arm movement in space: neurophysiological and computational approaches. Exp Brain Res, Suppl 22. Springer, Berlin

Hoenig JM, Heisey DM (2001) The abuse of power: the pervasive fallacy of power calulatons for data analysis. Am Stat 55:19–24

Hore J, Watts S, Vilis T (1992) Constraints on arm position when pointing in three dimensions: Donders' law and the Fick-gimbal strategy. J Neurophysiol 68:374–383

Krebs HI, Hogan N (2006) Therapeutic robotics: a technology push. Proc IEEE 94:1727–1738

Krebs HI, Volpe BT, Williams D, Celestino J, Charles SK, Lynch D, Hogan N (2007) Robot-aided neurorehabilitation: a robot for wrist rehabilitation. IEEE Trans Neural Syst Rehabil Eng 15:327–335

Lacquaniti F, Terzuolo CA, Viviani P (1983) The law relating kinematic and figural aspects of drawing movements. Acta Psychol 54:115–130

Latash ML, Scholz JP, Schoner G (2007) Toward a new theory of motor synergies. Mot Control 11:276–308

Leonard L, Sirkett D, Mullineux G, Giddins GEB, Miles AW (2005) Development of an in vivo method of wrist joint motion analysis. Clin Biomech 20:166–171

Li ZM, Kuxhaus L, Fisk JA, Christophel TH (2005) Coupling between wrist flexion–extension and radial–ulnar deviation. Clin Biomech 20:177–183

Liebermann DG, Biess A, Friedman J, Gielen CCAM, Flash T (2006) Intrinsic joint kinematic planning. I: reassessing the Listing's law constraint in the control of three-dimensional arm movements. Exp Brain Res 171:139–154

Masia L, Casadio M, Rodriguez NN, Morasso P, Giannoni P, Sandini G (2009) Adaptive training strategy of distal movements by means of a wrist-robot. In: 2nd International conference on advances in computer–human interactions, pp 227–233

Murray RM, Li Z, Sastry SS (1994) A Mathematical introduction to robotic manipulation. CRC Press, Boca Raton

Oldfield RC (1971) The assessment and analysis of handedness: the Edinburgh inventory. Neuropsychologia 9:97–114

Scholz JP, Schoner G (1999) The uncontrolled manifold concept: identifying control variable for a functional task. Exp Brain Res 126:289–306

Shadmehr R, Mussa-Ivaldi FA (1994) Adaptive representation of dynamics during learning of a motor task. J Neurosci 14:3208–3224

Soechting JF, Terzuolo CA (1987) Organization of arm movements in three-dimensional space. Wrist motion is piecewise planar. Neuroscience 23:53–61

Soechting JF, Buneo CA, Herrmann U, Flanders M (1995) Moving effortlessly on three dimensions: does Donders' law apply to arm movements? J Neurosci 15:6271–6280

Takahashi CD, Der-Yeghiaian L, Le V, Motiwala RR, Cramer SC (2008) Robot-based hand motor therapy after stokes. Brain 13:425–437

Trujillo-Ortiz, A. and R. Hernandez-Walls. (2003). powerMAOV1: Estimation of statistical power of a performed single-factor AMOVA. A MATLAB file. [WWW document]. URL http://www.mathworks.com/matlabcentral/fileexchange/

Tweed D, Vilis T (1990) Geometric relations of eye position and velocity vectors during saccades. Vis Res 30:111–127

Uno Y, Kawato M, Suzuki R (1989) Formation and control of optimal trajectory in human multijoint arm movement. Minimum torque-change model. Biol Cybern 61:89–101

Viviani P, Schneider R (1991) A developmental study of the relationship between geometry and kinematics in drawing movements. J Exp Psychol 12:198–218

Wong AMF (2004) Listing's law: clinical significance and implications for neural control. Surv Ophthalmol 49:563–575

Wu G et al. (2005) ISB recommendation on definitions of joint coordinate systems of various joints for the reporting of human joint motion—part II: shoulder, elbow, wrist and hand. J Biomech 38:981–992